

RECEIVED

APR 13 1999

J. P. SCHIFFER

Isolating the Thermal Degree of Freedom
in Nuclear Multifragmentation*

J. E. Viola, T. Lefort, K. Kwiatkowski¹, W.-c. Hsi, and L. Beaulieu
Department of Chemistry and IUCF, Indiana University, Bloomington, IN 47405

L. Pienkowski
Heavy Ion Laboratory, Warsaw University, Warsaw Poland

R.G. Korteling
Department of Chemistry, Simon Fraser University, Burnaby, B.C. V5A 1S6 Canada

R. Laforest, E. Martin, E. Ramakrishnan,
D. Rowland, A. Ruangma, E. Winchester and S.J. Yennello
Department of Chemistry and Cyclotron Lab, Texas A & M University, College Station, TX 77843

S. Gushue and L.P. Remsberg
Physics Division, Brookhaven National Laboratory, Upton, NY 11973

H. Breuer
Department of Physics, University of Maryland, College Park, MD 20740

B. Back
Physics Division, Argonne National Laboratory, 9700 S. Cass Avenue, Argonne, IL 60439

[To be published in *Proceedings of the Multifragmentation, Intl. Workshop XXVII on Gross Properties of Nuclei and Nuclear Excitations*, Hirschegg, Kleinwalsertal, Austria, 17-23 January 1999.]

*Research supported by the U.S. Department of Energy and National Science Foundation, the National Sciences and Engineering Research Council of Canada, the Robert A. Welch Foundation and Grant No. P03B 048 15 of the Polish State Committee for Scientific Research.

¹Present address: Los Alamos National Laboratory, Los Alamos, NM 87545

The submitted manuscript has been authored by a contractor of the U. S. Government under contract No. W-31-109-ENG-38. Accordingly, the U. S. Government retains a nonexclusive, royalty-free license to publish or reproduce the published form of this contribution, or allow others to do so, for U. S. Government purposes.

RECEIVED
OCT 19 1999
OSTI

DISCLAIMER

This report was prepared as an account of work sponsored by an agency of the United States Government. Neither the United States Government nor any agency thereof, nor any of their employees, make any warranty, express or implied, or assumes any legal liability or responsibility for the accuracy, completeness, or usefulness of any information, apparatus, product, or process disclosed, or represents that its use would not infringe privately owned rights. Reference herein to any specific commercial product, process, or service by trade name, trademark, manufacturer, or otherwise does not necessarily constitute or imply its endorsement, recommendation, or favoring by the United States Government or any agency thereof. The views and opinions of authors expressed herein do not necessarily state or reflect those of the United States Government or any agency thereof.

DISCLAIMER

Portions of this document may be illegible in electronic image products. Images are produced from the best available original document.

**ISOLATING THE THERMAL
DEGREE OF FREEDOM
IN NUCLEAR MULTIFRAGMENTATION**

V.E.VIOLA, T. LEFORT, K. KWIATKOWSKI,¹ W.-c. HSI,
and L. BEAULIEU

*Department of Chemistry and IUCF, Indiana University
Bloomington, IN 47405, USA*

L. PIENKOWSKI

Heavy Ion Laboratory, Warsaw University, 02 097 Warsaw, Poland

R.G. KORTELING

Simon Fraser University, Burnaby, B.C, V5A 1S6 Canada

R. LAFOREST, E. MARTIN, E. RAMAKRISHNAN, D. ROWLAND,
A. RUANGMA, E. WINCHESTER, and S.J. YENNELLO

*Department of Chemistry and Cyclotron Laboratory
Texas A & M University, College Station, TX 77843, USA*

S. GUSHUE and L.P. REMSBERG

Physics Division, Brookhaven National Laboratory, Upton, NY 11973 USA

H. BREUER

Department of Physics, University of Maryland, College Park, MD 20742, USA

B. BACK

Argonne National Laboratory, 9700 S. Cass Ave., Argonne, IL 60439, USA

Abstract

Multifragmentation studies induced by GeV light-ion beams permit investigation of the influence of intrinsic thermal properties of hot nuclear

¹present address: Los Alamos National Laboratory, Los Alamos, NM 87545

matter, with minimal interference from the compression/decompression cycle and rotational instabilities. We summarize recent results obtained with ^3He , proton and pion beams up to 15 GeV/c and present the initial results from a recent experiment with 8 GeV/c antiproton and pion beams. The results are compared with INC simulations coupled to EES and SMM models and the caloric curve for the ^3He data will also be discussed.

1 Introduction

Studies of nuclear multifragmentation have exposed a rich source of challenging new physics questions during recent years. Motivated by the desire to define the parameters of the nuclear equation of state, experimentalists have sought to resolve several crucial issues relevant to the properties of hot nuclear matter. Can equilibrated systems be clearly identified? Is there evidence for a liquid-gas phase transition, and if so, is it first or second order? What can the data tell us about nuclear compressibility? Is it possible to relate data from finite systems observed in the laboratory to the infinite systems that presumably occur in neutron stars? Many different physical effects – temperature, the compression/decompression cycle, rotational and shape degrees of freedom – can influence the probability for multifragmentation. Isolation of the thermal character of the multifragmentation process can be achieved most transparently via studies conducted with GeV light-ion beams, ideally hadrons. Both BUU[1] and INC[2] calculations indicate that such beams heat heavy target nuclei rapidly ($\tau \lesssim 20 \text{ fm}/c$), while at the same time providing minimal compression and imparting low average angular momenta ($\langle \ell \rangle \lesssim 20\hbar$) to the residue. Thus, the good news is that hadron-like beams suppress the effects of the compression/decompression cycle, rotational effects and the shape degree of freedom. The bad news is that the highly interesting phenomena associated with these effects, e.g., radial flow and neck emission, are not accessible via this approach and are pursued much more profitably with heavy-ion beams.

For hadron-like beams above about 3-4 GeV incident on heavy nuclei and INC[2, 3] calculations predict cross-sections of order 100 mb for residues with excitation energies in excess of the multifragmentation threshold, subsequently verified experimentally [4, 5, 6]. In addition, BUU[1] calculations indicate that the average entropy per nucleon becomes approximately constant after $\sim 30 \text{ fm}/c$, permitting a schematic separation of the reaction into fast cascade and subsequent decay stage(s). This serves as a rationale for the use of hybrid

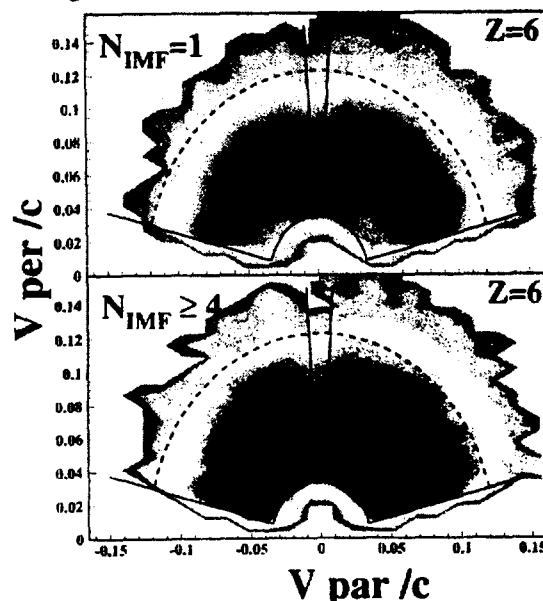
two-step calculations[7] for describing these reactions – although a unified theoretical description remains a highly desirable goal.

From an experimental point of view, hadron-like beams create only a single source of multifragmentation reactions. One of the remarkable features of these studies at GeV energies is that the multifragmentation events with the highest multiplicities are characterized by nearly isotropic IMF emission patterns. Fragment spectra for such events are concentrated at very low kinetic energies ($E/A \lesssim 5$ MeV/A), resembling a “soft explosion”. Longitudinal source velocities are typically $\lesssim 0.01c$, thus minimizing the kinematic distortion of the spectra and event patterns, as well as exposing nonequilibrium components in the observed yield. These features require a 4π symmetric detector with very low energy thresholds ($E/A \lesssim 1$ MeV) and good energy resolution. In the experiments reported here we have used the Indiana Silicon Sphere (ISiS) 4π detector array, which consists of 162 gas-ion chamber/500 μm silicon/28 mm CsI telescopes arranged in a spherical geometry and covering 74% of 4π [8].

2 The Case for Thermalization and Expansion

The initial experimental test for equilibration, a necessary condition for a nucleus undergoing a phase transition, is that the fragments must be emitted isotropically in the source frame. In Fig. 1 we show constant invariant cross

Fig. 1. Invariant cross sections for ^{12}C fragments emitted in the 8 GeV/c $\pi^- + ^{197}\text{Au}$ reaction, gated on IMF multiplicity, $N_{\text{IMF}}=1$ and $N_{\text{IMF}} \geq 4$. Solid lines define detector acceptance; fragments enclosed within dashed line are defined as thermal

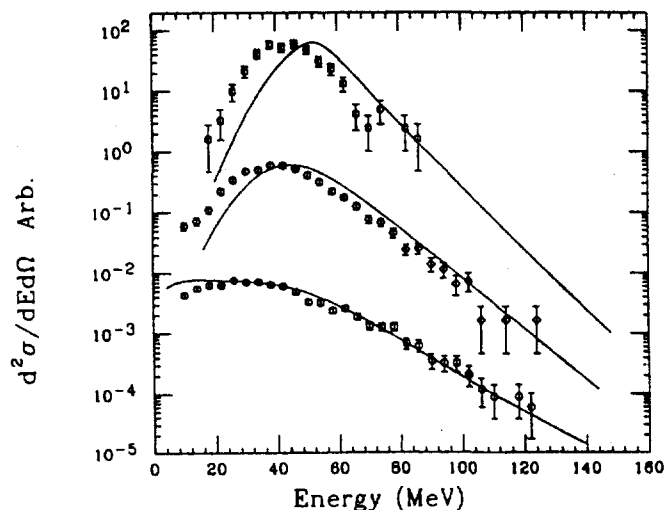


sections (rapidity) plots for carbon fragments emitted in the 8.1 GeV/c π^- and ^{197}Au reaction, as a function of observed IMF multiplicity, N_{IMF} . One

observes that for the least violent events ($N_{IMF} = 1$), the rapidity distributions are consistent with a low source velocity, but are somewhat forward-focussed, suggesting contributions from nonequilibrium processes. As the observed multiplicity increases, there is little change in the source velocity, while the rapidity pattern shifts increasingly towards greater isotropy and lower fragment velocities. This behavior is a general feature of all IMFs with $Z \geq 6$ and has been observed in several similar systems with GeV ^3He and proton beams[6, 9]. While this confirms that the momenta of the nucleons in the hot residue are randomized, the question of equilibration, of course, remains open. Nonetheless, it is apparent in Fig. 1 that these highly relativistic beams produce a class of events that decay isotropically and are characterized by unusually soft (sub-Coulomb) energy spectra.

The systematic shift in the spectra toward lower energies as a function of increasing total observed charge Z_{obs} is shown in Fig. 2 for carbon fragments emitted in the 4.8 GeV $^3\text{He} + ^{197}\text{Au}$ reaction. The observed evolution of the spectra suggests that expansion may play an important role in producing the disintegration mechanism. To investigate this possibility, two-component moving-source fits[10] have been applied to the data for $Z \geq 5$ fragments as a function of observed IMF multiplicity. From the Coulomb parameters, k_c , derived from such fits, it is possible to estimate the corresponding relative volume V and density ρ , since $k_c \propto 1/V^{1/3} \propto \rho^{1/3}$. In performing these fits, it was recognized that in a sequential decay scenario, the charge of the emitting source decreases at each step, thus lowering the Coulomb field and producing less energetic fragments. Thus, it was assumed that the observed fragment was the final step in a de-excitation chain and that the charge of the corresponding residue was the difference between that of the ^{197}Au target and all remaining observed charge, Z_{obs} , in the reaction; i.e. $Z_{source} = 79 - Z_{obs} + Z_{IMF}$. In this way the extracted values of k_c are maximized, producing an upper limit on the density.

Fig. 2. Laboratory energy spectra of carbon fragments for 4.8 GeV $^3\text{He} + ^{197}\text{Au}$ reactions at 119° . Points correspond to experimental data; line is the result of INC/EES calculations. Gating conditions on Z_{obs} are 1-10 (top); 11-20 (middle) and 51-60 (bottom).



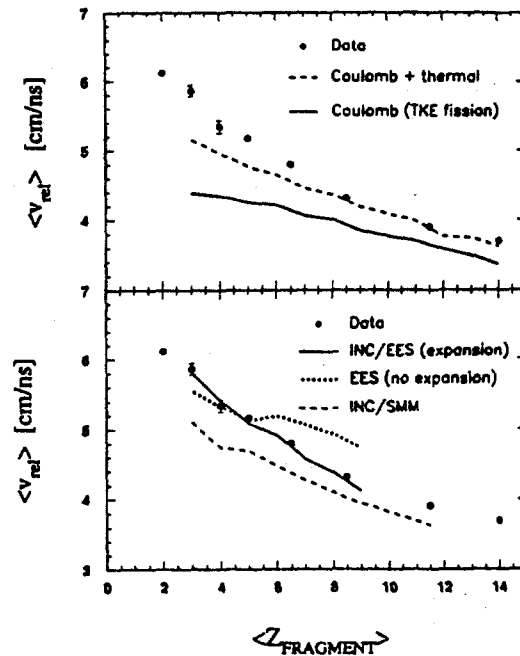
This analysis yields decreasing values of ρ/ρ_0 with increasing N_{IMF} that become constant near $\rho/\rho_0 \leq 0.3-0.4$ for $N_{IMF} \geq 4$, corresponding to an excitation energy of about 750 MeV[4]. This provides a direct rationale for a breakup density of $\rho/\rho_0 \lesssim 1/3$ and is consistent with the breakup densities required to fit the data with EES[11] and SMM[12, 13] multifragmentation model simulations. This is indicated by the qualitative trends of the solid lines in Fig. 2, which are based upon EES calculations. Sequential statistical models cannot reproduce this effect.

3 The Breakup Mechanism(s): Time Scales

Another issue central to the identification of a phase transition in hot nuclei is the time evolution of the hot residue. To what extent are the residue mass and energy depleted by pre-breakup phenomena such as coalescence and preequilibrium emission? Are the observed high multiplicity, sub-Coulomb events the product of a sequential or a simultaneous disintegration? In order to address these questions, both large- and small-angle IMF-IMF velocity correlations have been performed on the 4.8 GeV $^3\text{He} + ^{197}\text{Au}$ data. Large-angle relative velocity correlations are sensitive to the size and temperature of the emitting source and can be used to trace the time-temperature evolution of the residue[14]. Small-angle reduced velocity correlations probe the breakup time scale. Details of the analyses reported here are contained in [15, 16].

In Fig. 3 the average relative velocities are shown as a function of IMF

Fig. 3. Points: average fragment-fragment large-angle relative velocities as a function of fragment charge. Upper panel: solid line gives prediction of fission TKE systematics; dashed line is for TKE systematics from a source at $T=5$ MeV. Lower panel: INC/EES model for $\rho/\rho_0 = 1/3$ (solid line), INC/EES model for $\rho/\rho_0 = 1$ (dotted line) and INC/EES model for $\rho/\rho_0 = 1$.

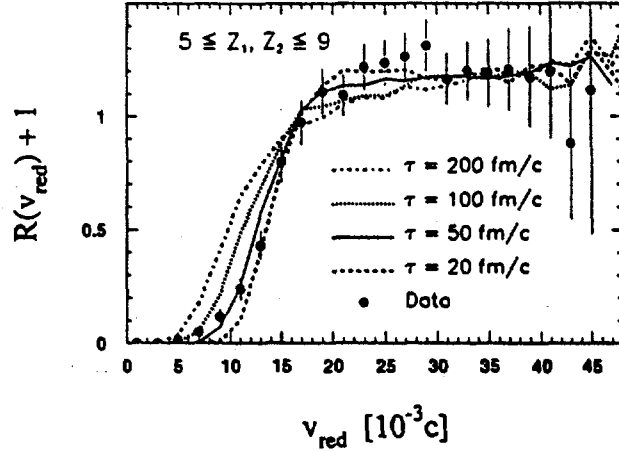


charge for the large-angle correlations. Only fragments emitted at angles greater than 32° and with kinetic energies $E/A \leq 10$ MeV were included in the data set. In the top frame of Fig. 3 the data are compared with predictions of fission kinetic-energy systematics[17] to provide a baseline for Coulomb effects from highly stretched nuclear matter. The solid line shows the systematics for a residual nucleus at $T=0$ and the upper curve for $T=5$ MeV. For the heavier fragments the calculation for a hot residue describes the data relatively well. However, for fragments with $Z \lesssim 6$, the fission systematics underpredict the data, which is also true of statistical model simulations described below.

In the bottom frame of Fig. 3, relative velocity results are compared with two hybrid simulations; both of which use the residue mass and excitation energy distributions predicted by intranuclear cascade calculations as input[18]. The solid line shows the results of an INC/EES simulation based on the time-dependent expanding emitting source model and the dashed line gives the prediction for an INC/SMM model that employs instantaneous breakup. Both models assume a breakup density of $\rho/\rho_0 \sim 1/3$ and describe the data for heavier IMFs relatively well. However, for the lighter IMFs, only the INC/EES model, which includes emission during expansion, accounts for the data. The effect of expansion is also shown by the dotted line in Fig. 3, where the case of no expansion ($\rho/\rho_0 = 1$) in the INC/EES model is seen to be in strong disagreement with the data. Thus, the large-angle correlations are consistent with a scenario in which, on average, light IMFs are emitted in a time-dependent fashion from a hotter, more dense source during expansion, whereas heavy IMFs originate from a dilute source with $\rho/\rho_0 \lesssim 1/3$ later in the time evolution of the reaction.

In order to evaluate the time scale for breakup in the final stages of the reaction, small-angle reduced-velocity correlations have been performed on the 4.8 GeV ${}^3\text{He} + {}^{197}\text{Au}$ data. Since the strongest evidence for expansion and thermal multifragmentation is provided by the high yield of sub-Coulomb IMFs found in the spectra of the most violent events[6, 10], we have focused our analysis on those events with energies, $E_{\text{IMF}}/A \leq 3$ MeV per nucleon. These results are shown in Fig. 4 for high multiplicity events from the 4.8 GeV ${}^3\text{He} + {}^{197}\text{Au}$ reaction. Data are for $Z=5-9$ fragments, which account for about 50 mb of total cross section. Also shown in Fig. 4 are simulations based on the N-body Coulomb-trajectory code of Glasmacher[19]. Here we assume $\rho/\rho_0 = 0.25$, a value of $Z=12$ for the heaviest residue in the ensemble, and random placement of the heaviest residue in the breakup volume. With values of the heaviest residue greater than $Z \geq 20$, it is not possible to describe the shape of experimental data. These assumptions account for the fragment multiplicity,

Fig. 4. Reduced relative velocity correlations as a function of reduced velocity for the 4.8 GeV $^3\text{He} + ^{197}\text{Au}$ reaction (points). Data were selected for pairs of events in which $M_{th} \geq 11$ and $(E/A)_{IMF} = 0.7 - 3.0$ MeV and are shown for $Z=5-9$ fragments. Lines are results of an N-body simulation with $\rho/\rho_0 = 0.25$ and maximum residue size, $A_{res}=12$. Time scales are indicated on figure.



charge and kinetic energy distributions. Breakup time scales of 20, 50, 100 and 200 fm/c are indicated on the figure. The comparisons strongly favor a very short breakup time, $\tau \sim 20 - 50$ fm/c, thus supporting a near-simultaneous origin of these multifragment events. Thus, the picture that is suggested by the IMF-IMF correlation data and simulations contains both time-dependent and simultaneous emission phases. Light fragments appear to be emitted during the early stages of the reaction from an expanding cooling source. For those residues formed at sufficiently high temperatures, expansion then leads to simultaneous breakup of the system when a density of $\rho/\rho_0 \lesssim 1/3$ is reached. These latter events then represent the most likely candidates for a phase transition.

4 Excitation Energy: Enhancement with Antiprotons

The thermal character and short apparent breakup times associated with the multifragmentation events observed in these studies suggest a possible interpretation in terms of a phase transition. To investigate this possibility, we have constructed the "caloric curve" [20] for the 4.8 GeV ^3He -induced reactions on ^{nat}Ag and ^{197}Au . Excitation energies were derived event-by-event for the thermal component of the spectra, following procedures described in [4]. The distribution of E^*/A values extends up to $E^*/A \simeq 10$ MeV/nucleon for both systems. Comparison with predictions of an INC calculation [18] show that the simulation overpredicts the extracted excitation energies by about 15% at the upper end of the distribution. However, if nonequilibrium emission is included in the energy sum ($E/A \leq 30$ MeV), the agreement with INC im-

proves significantly – which is consistent since the INC code does not account for equilibrium emission.

Temperatures have been derived using the double-isotope ratio method, with the $^2,3\text{H}/^3,4\text{He}$ isotopes serving as the thermometer[22]. The resultant “caloric curve” is shown in Fig. 5. The heating curves for both ^{nat}Ag and ^{197}Au are nearly identical and no plateau is seen in the data, although a distinct slope change is indicated near $E^*/A \sim 2\text{-}3$ MeV. The data are compared with the EES model in the left frame and the SMM model on the right, as well as the simple thermal expectations based on a level density parameter $a=A/11$ MeV $^{-1}$ (dotted line). The full model calculation is given by the dashed line and the model filtered through the ISiS detector acceptance by the solid line. Both models, which assume a phase transition near $E^*/A \sim 5$ MeV, are in relatively good accord with the data based on thermal ejectiles only. It should be noted, however, that model isotope-ratio temperatures do not necessarily coincide with the thermodynamic temperatures for a given excitation energy/nucleon (dot-dashed line in SMM calculation).

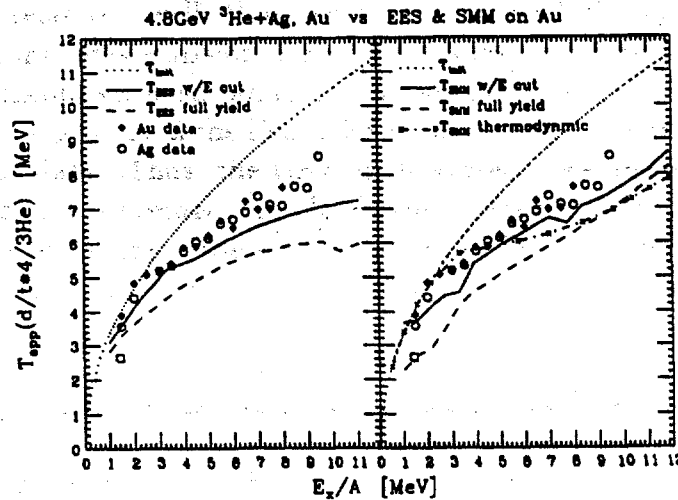


Fig. 5. Caloric curve for 4.8 GeV $^3\text{He} + ^{nat}\text{Ag}, ^{197}\text{Au}$ reactions. Temperatures are determined from $^2,3\text{H}/^3,4\text{He}$ double isotope ratios and excitation energy per residue nucleon from reconstructed events. Left frame compares with EES model; right curve compares with SMM model with detector cuts imposed on theory (solid lines).

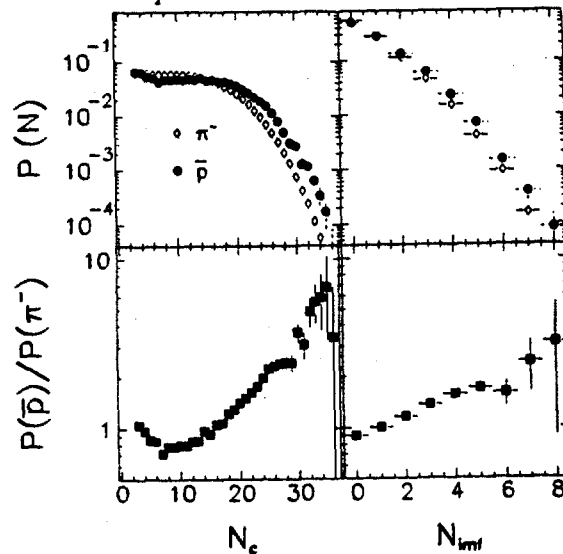
Qualitatively, the caloric curve of Fig. 5 is in agreement with both model predictions and expectations of a liquid undergoing a phase transition. Two questions immediately arise. First, are the isotope-ratios a valid gauge of the temperature of the hot source? This remains an open question. Second, what

happens at higher excitation energies; i.e., can evidence for vaporization be found? The use of light-ion and hadron beams to reach higher excitation energies is limited due to the observed saturation in deposition energy that occurs for beams above about 4-5 GeV kinetic energy[5, 23]. This saturation is presumably linked to the loss of retained energy in the target nucleus due to transparency effects as the beam energy increases.

In an effort to extend the heating curve to higher excitation energies, we have recently studied antiproton-induced reactions with the ISiS array at the Brookhaven AGS. INC calculations predict that for antiprotons above about 5 GeV/c momentum, the excitation-energy distribution of the excited residues extends to significantly higher values than for proton- and pion-induced reactions[3].

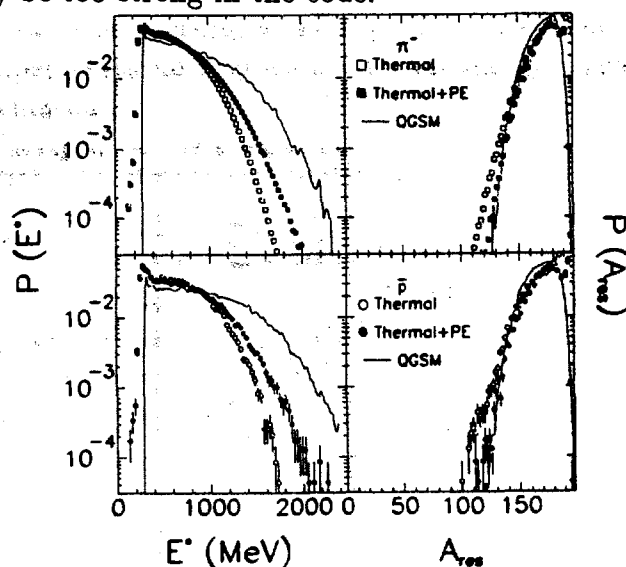
The simulations suggest that a 20-40% enhancement is the upper values of E^*/A might be observed. The experiment was performed with a tagged beam of 8 GeV π^- ($\sim 98\%$), K^- ($\sim 1\%$) and \bar{p} ($\sim 1\%$). Approximately 25,000 \bar{p} events and $2.5 \times 10^6 \pi^-$ events were observed with one or more IMFs. The observed multiplicity distributions are shown for total charged particles (N_{CP}) and IMFs (N_{IMF}) in the upper panels of Fig. 6. The data demonstrate a clear enhancement of high multiplicity events for the \bar{p} beam relative to the π^- beam. (It has previously been shown that the π^- and proton beams yield identical multiplicity distributions[21]). More apparent is the ratio of probabilities for the two beams, shown in the lower panels of Fig. 6. Here one sees a factor of at least three increase in the probability for the highest IMF multiplicities with the \bar{p} beam. The total charged-particle multiplicities are even more enhanced, in part due to more fast particles in those \bar{p} -induced events.

Fig. 6. Top panels: Total charged particle (left) and IMF (right) multiplicity distributions for bombardment of 8 GeV/c π^- (open points) and \bar{p} (closed points). Lower panels: Ratios of \bar{p} to π^- probabilities as a function of total charged particle (left) and IMF (right) multiplicity.



In Fig. 7 the derived excitation energy and mass distributions are compared with the INC predictions for 8 GeV/c π^- and \bar{p} beams, respectively. Two assumptions are shown for the values derived from the data. Open squares include only thermal particles, which we define as protons with kinetic energy $E < 30$ MeV and all other fragments with $E \leq 9.0Z + 40$ MeV (as indicated by the area enclosed within the dotted line in Fig. 1). For the solid squares the acceptance is relaxed to include all fragments with $E/A \leq 30$ MeV. Qualitatively, the INC calculation predicts the observed enhancement of high excitation energies with \bar{p} relative to the hadron beams. However, on an absolute basis, the INC overestimates the maximum excitation energies significantly, although the agreement with the mass distributions derived from the experiment is reasonable. This suggests that the reabsorption of secondary pions during the cascade may be too strong in the code.

Fig. 7. Excitation energy (right) and residue mass distributions (left) for 8 GeV/c π^- (top) and \bar{p} bombardment of ^{197}Au . Open points show thermal energies only, solid points include nonequilibrium emission and lines are prediction of INC calculation.



5 Summary

In summary, studies of GeV antiproton, hadron- and ^3He -induced multifragmentation reactions have led to the following interpretation of these reactions. Initially, the nucleus is rapidly heated via hard N-N collisions, multiple baryonic resonance excitations and pion reabsorption, leading to deposition energies in excess of ~ 10 MeV/residue nucleon. During the latter stages of the fast cascade and subsequent expansion/cooling phase, nonequilibrium LCPs and IMFs are emitted from sources that are hotter and more dense than at breakup. Examination of the sub-Coulomb part of the IMF breakup spectrum suggests a "soft explosion" of the hot, expanded residue for which the breakup time is $\tau \lesssim 20\text{-}50$ fm/c. The caloric curve derived from the thermal part of the ejectile spectra exhibits a slope change near $E^*/A \sim 2\text{-}3$ MeV, but contin-

ues to increase gradually up to $E^*/A \sim 10$ MeV. This behavior is consistent with both EES and SMM multifragmentation models. Finally, recent studies with 8 GeV/c \bar{p} and π^- beams indicate that antiprotons in this momentum range may provide the optimum case for investigating thermal behavior in multifragmentation reactions.

References

- [1] G. Wang *et al.*, Phys. Rev. C. **53**, 1811 (1996).
- [2] J. Cugnon, Nucl. Phys. **462**, 751 (1987).
- [3] V. Toneev *et al.*, Nucl. Phys. A **519**, 463c (1990).
- [4] K. Kwiatkowski *et al.*, Phys. Lett. B **423**, 21 (1998)
- [5] K.B. Morley *et al.*, Phys. Rev. C **54**, 737 (1996)
- [6] E. Renshaw Foxford, K. Kwiatkowski, V.E. Viola, W. Bauer, and P. Danielewicz, Phys. Rev. C **54**, 749 (1996).
- [7] K. Kwiatkowski, W. A. Friedman, *et al.*, Phys. Rev. C **49**, 1516 (1994).
- [8] K. Kwiatkowski *et al.*, Nucl. Instr. Meth. A **360**, 571 (1995).
- [9] V. Audeyev *et al.*, Eur. Phys. J. A, **75**, (1998).
- [10] D.S. Bracken, Ph.D. Thesis, Indiana University, 1996 (unpublished).
- [11] W.A. Friedman, Phys. Rev. C **42**, 667 (1990).
- [12] A. Botvina, A.S. Iljinov and I.N. Mishustin, Nucl. Phys. A **507**, 649 (1990).
- [13] J. P. Bondorf *et al.*, Phys. Rep. **257**, 133 (1995).
- [14] R. Tröckel *et al.*, Phys. Rev. Lett. **59**, 2844 (1987).
- [15] G. Wang *et al.*, Phys. Lett. B **393**, 290(1997).
- [16] G. Wang *et al.*, Phys. Rev C **57** R2786 (1998).
- [17] V. E. Viola *et al.*, Phys. Rev. C **31**, 1550 (1985).
- [18] Y. Yariv and Z. Fraenkel, Phys. Rev. C **20**, 2227 (1979); **24**, 488 (1981).
- [19] T. Glasmacher *et al.*, Phys. Rev. C **50**, 952 (1994).
- [20] J. Pochodzalla *et al.*, Phys. Rev. Lett. **75**, 1040 (1995).
- [21] W.-c. Hsi *et al.*, Phys. Rev. Lett. **79**, 817 (1997).
- [22] J. Albergo *et al.*, Nuovo Cim. **89A**, 1, 1985.
- [23] D. Strottman and W.R. Gibbs, Phys. Lett. B **149**, 288 (1984).